

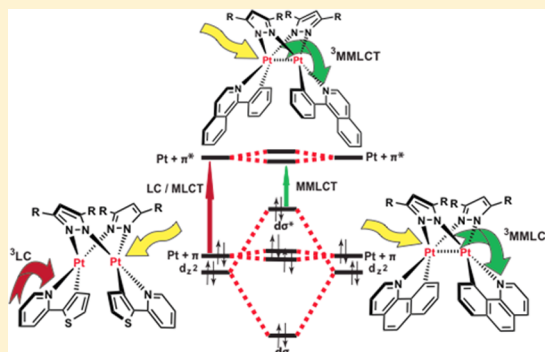
Charge-Transfer and Ligand-Localized Photophysics in Luminescent Cyclometalated Pyrazolate-Bridged Dinuclear Platinum(II) Complexes

Arnab Chakraborty, Joseph C. Deaton, Alexandre Haefele, and Felix N. Castellano*

Department of Chemistry and Center for Photochemical Sciences, Bowling Green State University, Bowling Green, Ohio 43403, United States

S Supporting Information

ABSTRACT: We present the synthesis, photophysical characterization, and electrochemistry of three series of cyclometalated binuclear platinum(II) complexes, each bridged by two 3,5-disubstituted pyrazolate ligands (μ -R₂pz). These neutral compounds have the general formula [C[^]NPt(μ -R₂pz)]₂, where C[^]N is a cyclometalating ligand corresponding to 2-(2'-thienyl)pyridine (thpy), 1-phenylisoquinoline (piq), or 7,8-benzoquinoline (bzq) with R = H, Me, ⁱPr, Ph, corresponding to series I–III dimers, respectively. Systematic variation of the cyclometalating ligands in addition to the bridging pyrazolates renders colorful structures exhibiting a range of electrochemical and spectroscopic behavior with absorption and photoluminescence properties tuned over a wide portion of the visible spectrum. Steric bulk introduced into the 3,5-positions on the pz bridges readily modulates intramolecular d⁸–d⁸ metal–metal σ interactions strongly affecting the frontier orbitals' electronic structure, manifested by changes in absorption and emission energy, excited-state lifetime, and photoluminescence quantum yield. Cyclic voltammetry revealed the presence of two very closely spaced reversible C[^]N ligand-based reductions ranging between –1.97 and –2.56 V vs Fc⁺/Fc, and the first metal–metal-centered oxidation wave was found to be reversible in dichloromethane and irreversible in coordinating THF in most instances. All the complexes of series I displayed triplet ligand-localized excited states at all temperatures, while an increase of steric bulk in the pz bridge in the two other molecular series resulted in a variation of photophysical behavior ranging from charge transfer to ligand localized, including admixture behavior.



INTRODUCTION

Cyclometalated coordination compounds of transition metals, particularly square-planar complexes of platinum(II) and palladium(II), have generated research interest for their numerous potential applications in addition to fundamental contributions in molecular materials. Such molecules have been used as photocatalysts,^{1–4} optoelectronic devices,^{5–10} cyanogen halide detection,¹¹ cation sensing,^{12,13} and pH sensing,^{14,15} as well as for DNA applications,^{16,17} as metallomesogens,^{18,19} and as anticancer agents.²⁰ All of these multidisciplinary applications consequently attracted substantial research interest toward extensive photophysical investigations on mononuclear cyclometalated Pt(II) complexes.^{21–39} The strong σ -donating ability of the cyclometalating ligands results in large d-orbital splitting effectively inactivating ligand field states, rendering strongly emissive molecules. The origin of emission in such mononuclear cyclometalated Pt(II) complexes generally results from ligand-centered (LC), ligand-to-ligand charge-transfer (LLCT), and/or metal-to-ligand charge transfer (MLCT) excited states.

Binuclear transition-metal complexes based on Pt(II) have also generated profound interest because of their intriguing photophysical properties.^{6,40–48} In particular, the rich excited-

state chemistry of the binuclear [Pt₂(μ -P₂O₅H₂)₄]^{4–} has been reported in the literature,⁴⁹ while there are numerous related chromophores that display changes in their photophysical properties with variation of ancillary and charge transfer ligands.^{33,50–55} In addition to Pt, there have been several reported studies on binuclear complexes of Pd and Ir.^{56–59} In select binuclear Pt(II) complexes, the d_{z²} orbital of each platinum center is forced to σ overlap and this interaction gives rise to filled d σ and d σ^* orbitals. This electronic structure effectively transforms high-energy absorbing mononuclear structures into colorful dinuclear molecules exhibiting reversible metal–metal-based oxidations with riveting photophysics.^{60–63} When the metal–metal coupling is sufficient, the photophysical properties can be considered to result from metal–metal-to-ligand charge transfer (MMLCT) excited states, involving charge transfer between a filled Pt–Pt d σ^* orbital and a ligand-localized vacant π^* orbital on the cyclometalating ligand (Figure 1).

Thompson and co-workers previously reported a series of binuclear platinum(II) complexes with 2-(2,4-difluorophenyl)-

Received: April 3, 2013

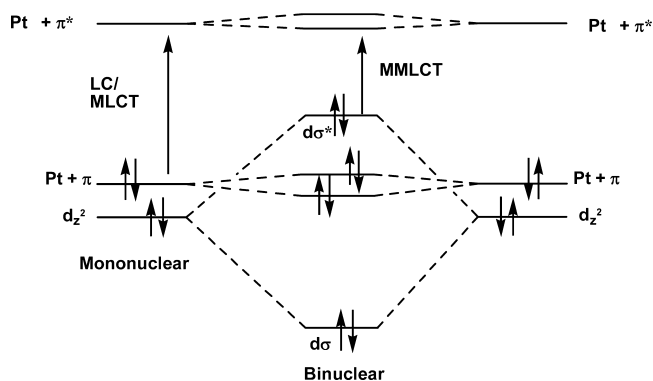


Figure 1. Simplified molecular orbital diagram illustrating the d^8 – d^8 interaction in cofacial dinuclear Pt(II) complexes.

pyridyl as the C[^]N ligand and showed that the photophysical properties of such platinum dimers can be readily tuned by introducing steric bulk in the bridging pyrazolate ligands.⁵⁰ In another report, the same group showed that such complexes can be used as phosphorescent dopants in OLEDs.⁶⁴ Recently there has been increasing interest in these classes of complexes in both ground- and excited-state properties.^{65,66} For example, an investigation of the temperature-dependent spectral and photophysical properties in $[\text{Pt}(\text{ppy})(\mu\text{-Ph}_2\text{pz})_2]_2$ was recently reported in addition to its solid-state thermochromic behavior.⁶⁷

In the present contribution we report the synthesis, photophysical characterization, and electrochemistry of an array of pyrazolate-bridged cyclometalated dinuclear platinum(II) complexes. All these complexes are emissive at both 77 K and room temperature. Here we have investigated how the systematic variation of cyclometalating ligand and the bridging pyrazolates affects the photophysical properties of these complexes. The bridging pyrazolates provide a framework to initiate metal–metal interactions in the ground-state A-frame geometry, where the extent of this interaction is controlled by the bulkiness introduced in the 3- and 5-positions of the bridging pyrazolates (Figure 2). Three series of platinum dimers were synthesized by using 2-(2'-thienyl)pyridine (thpy; series I), 1-phenylisoquinoline (piq; series II) and 7,8-benzoquinoline (bzq; series III) as the cyclometalating ligands and in each series methyl-, isopropyl-, and phenyl-disubstituted pyrazolates were used as bridging ligands in order to evaluate the effect of steric strain on the resultant photophysical

properties. A range of photophysical behavior was observed, including ligand-centered phosphorescence and charge-transfer photoluminescence, as well as admixtures of these two extremes.

RESULTS AND DISCUSSION

Syntheses and Structural Characterization. The intermediate cyclometalated dichloro-bridged platinum(II) dimers were prepared following a literature procedure with slight modification.³³ Instead of directly refluxing K_2PtCl_4 with the desired cyclometalating ligand, the precursor $\text{Pt}(\text{DMSO})_2\text{Cl}_2$ was substituted and refluxed in a mixture of 2-ethoxyethanol and water (3:1) (Scheme 1). This reaction proceeds without the formation of platinum black, which is often obtained when K_2PtCl_4 is utilized. The subsequent pyrazolate-bridged dimers were synthesized in a manner analogous to that previously developed in our laboratory.⁶⁷ In all instances, satisfactory mass spectra, elemental analyses or HR-MS spectra, and ^1H NMR data were obtained for each newly synthesized Pt(II) dimer. Almost all of these dimers were isolated as a mixture of *cis* and *trans* isomers with respect to the relative orientation of the two C[^]N ligands, and the *trans* form was the major product with a *trans*:*cis* ratio of ~ 2 :1. This is not surprising, as we have already described an identical isomerism in the analogous 2-phenylpyridine-containing molecules,⁶⁷ which is easily confirmed through ^1H NMR.

The ^1H NMR spectra of *trans*- $[\text{Pt}(\text{thpy})(\mu\text{-Me}_2\text{pz})_2]_2$ (**1b**) and *cis/trans* $[\text{Pt}(\text{thpy})(\mu\text{-H}_2\text{pz})_2]_2$ (**1a**) are presented in Figure 3 and serve as representative examples for *cis/trans* ^1H NMR assignments in these classes of molecules. The ^1H NMR spectrum of compound **1b**, which was obtained as the pure *trans* isomer, shows only one signal for each of the characteristic pairs of protons 1–3 (Figure 3A). Because of the presence of a C_2 symmetry axis in the *trans* isomers, these protons are magnetically equivalent and have identical chemical shifts. In contrast, this symmetry axis is not present in the *cis* isomers, being replaced by a plane of symmetry passing through the two pyrazolate moieties. This change in symmetry revealed in the *cis* isomers implies that the two cyclometalating ligands remain magnetically equivalent (but with different chemical shifts with respect to the *trans* isomers) and the two pyrazolates become chemically distinguishable. This *cis/trans* effect is most visible on the signal corresponding to the pyrazolate proton 2 in the ^1H NMR spectrum of the mixture of *cis/trans*-**1a** (Figure 3B). Only one triplet, at 6.5 ppm, is observed for the *trans*

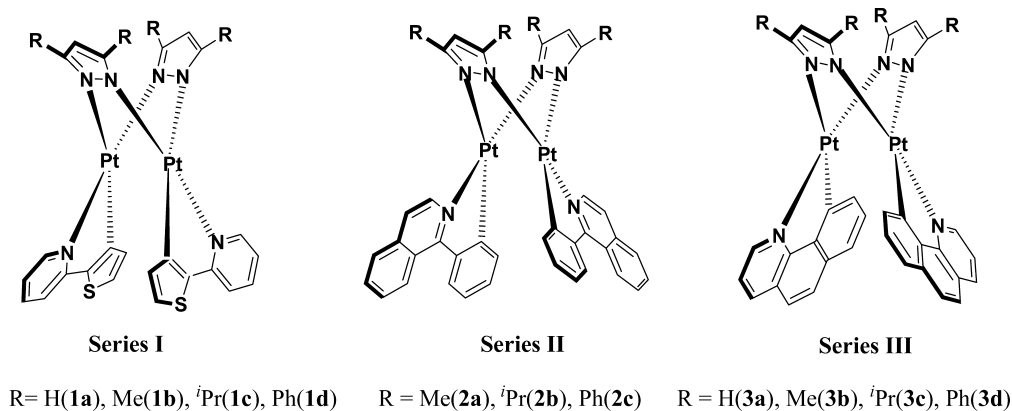


Figure 2. Structures of the three series of pyrazolate-bridged dinuclear Pt(II) complexes under investigation.

Scheme 1. Synthetic Route to Producing Dinuclear Pt(II) Complexes of Series I–III

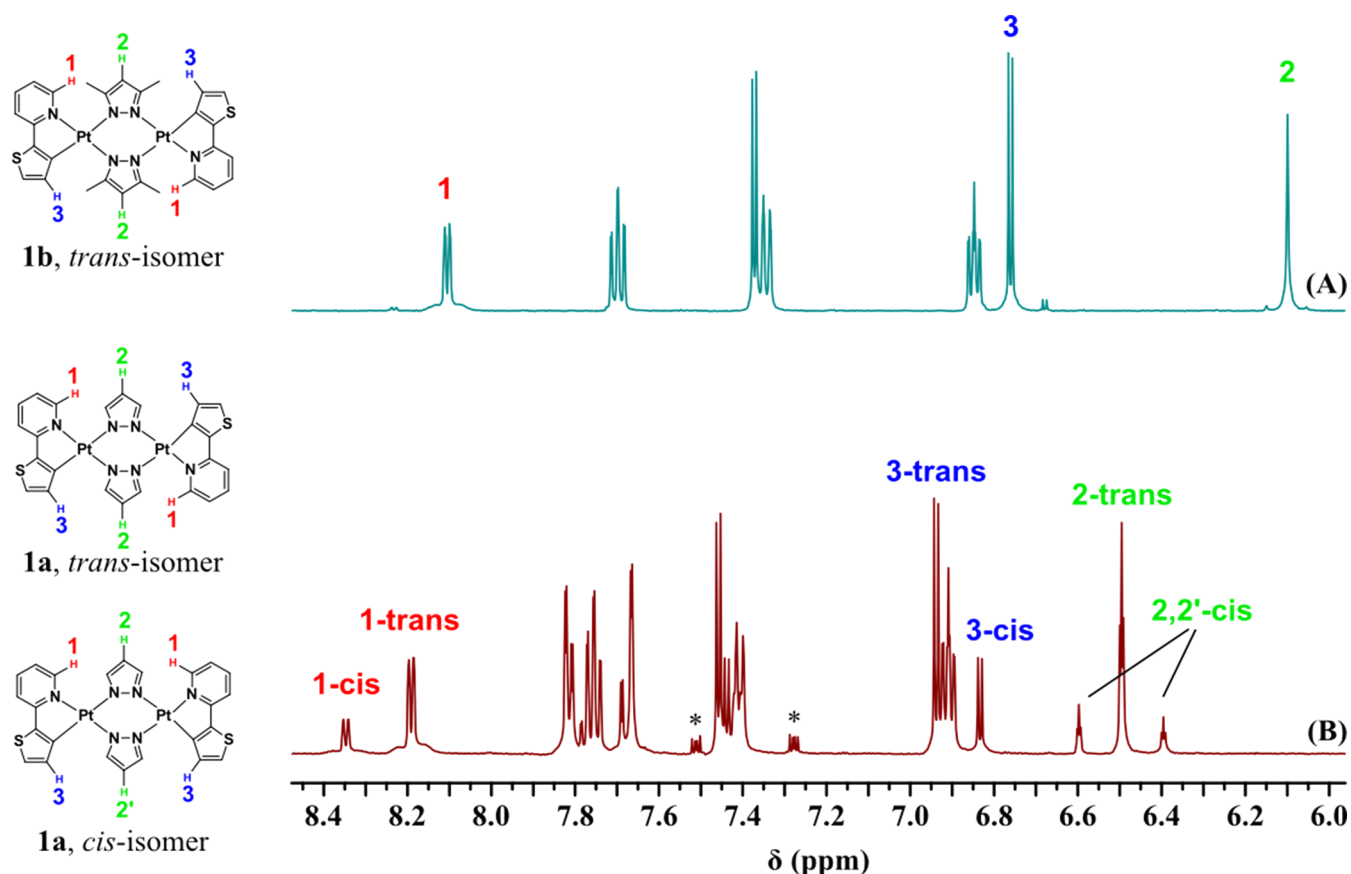
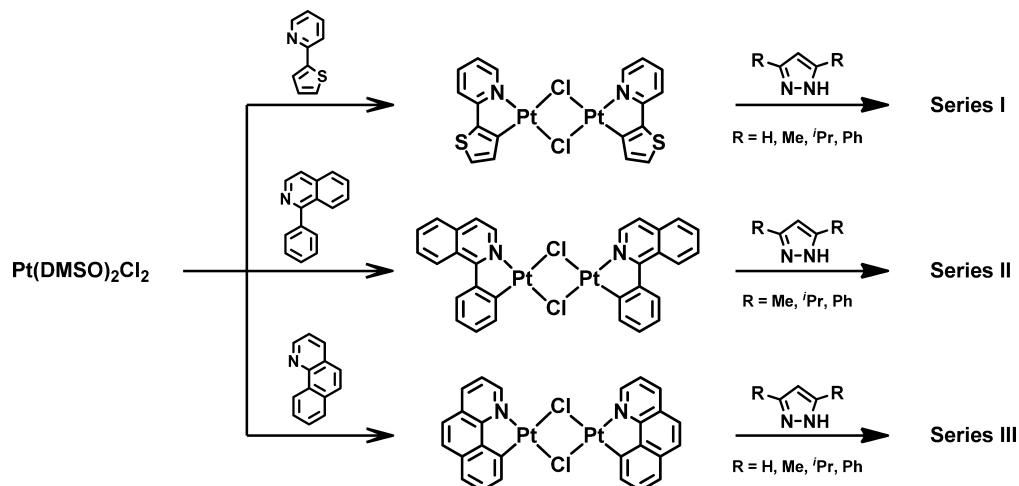


Figure 3. ^1H NMR spectra of **1b** (A) and **1a** (B) focusing only on the aromatic region recorded in CD_2Cl_2 . Labeled protons 1–3 are distinguishing signals corresponding to one proton in the pyridyl, pyrazolyl, and thienyl moieties respectively, while the asterisks (*) correspond to peaks from the residual 1,2-dichlorobenzene solvent. The structures of these associated isomers are presented for clarity.

isomer, whereas two triplets at 6.4 and 6.6 ppm are observed for the *cis* isomer, illustrating the difference in magnetic environment experienced by the two pyrazolate moieties. Protons 3 and 1 also produce different signals for the *cis* and *trans* isomers, the latter being used to determine the actual *cis/trans* isomer ratio. Similar NMR patterns were observed for all other Pt dimers investigated herein, when obtained as a mixture of *cis* and *trans* isomers.

Electrochemistry. Cyclic voltammetry (CV) and differential pulse voltammetry (DPV) were both utilized to evaluate

the redox potentials and electrochemical reversibility of the newly synthesized Pt(II) dimers. In all instances these measurements took place under a dry and inert atmosphere provided by a glovebox. The coordinating solvents included acetonitrile, 1/1 acetonitrile/toluene, and THF, selected to provide appropriate solubility and electrochemical potential measurement windows for both oxidations and reductions, along with noncoordinating CH_2Cl_2 , which was able to reveal metal–metal-based reversible oxidations in several instances. Peak potentials (E_{pa} or E_{pc}) were measured by DPV because

this method was necessary in instances where the redox couples were irreversible. The redox potentials obtained for all of the Pt(II) complexes under investigation are collected in Table 1.

Table 1. Electrochemical Data for the Platinum(II) Dimers^a

complex	$E_{1/2}(\text{ox})^b$ (V)	$E_{1/2}(\text{ox})^d$ (V)	$E_{1/2}(\text{red})$ (V)
1a	c	0.59 ^{ir}	-2.39 ^e
1b	0.50 ^{ir}	0.51 ^{ir}	-2.41 ^r , -2.52 ^e
1c	0.41 ^r	0.48 ^{ir}	-2.41 ^r , -2.55 ^e
1d	0.42 ^r	0.45 ^{ir}	-2.38 ^r , -2.56 ^e
2a	0.42 ^{ir}	0.48 ^{ir}	-2.00 ^r , -2.10 ^f
2b	0.35 ^r	0.43 ^{ir}	-1.98 ^r , -2.11 ^f
2c	0.33 ^r	0.36 ^{ir}	-1.97 ^r , -2.08 ^f
3a	c	0.53 ^{ir}	-2.21 ^{ir} ^e
3b	0.46 ^r	0.48 ^{ir}	-2.24 ^{ir} , -2.33 ^e
3c	0.37 ^{ir}	0.44 ^{ir}	-2.27 ^{ir} , -2.37 ^e
3d	0.38 ^r	0.38 ^{ir}	-2.21 ^{ir} , -2.37 ^e

^aAll measurements were performed with 0.1 M TBAPF₆ as the supporting electrolyte, and potentials are given vs the Fc⁺/Fc couple. ir = irreversible, and r = reversible. ^bMeasured in DCM. ^cCould not be measured due to rapid decomposition in DCM. ^dMeasured in THF. ^eMeasured in 1/1 acetonitrile/toluene. ^fMeasured in acetonitrile.

All the platinum dimers in series I and II exhibited two very closely spaced one-electron reductions, with the exception of 1a, where the first reduction is completely reversible. The complexes of series III are unique in the fact that each molecule exhibited electrochemically irreversible one-electron reductions. This is not too surprising, given that similar observations have been reported for mononuclear platinum(II) complexes bearing 7,8-benzoquinoline C[^]N ligands. Among the several square-planar cyclometalated platinum(II) complexes reported by Thompson and co-workers, it was seen only in the case of bzqPt(dpm) that the ligand-based reduction became irreversible. It is believed that the rigid planarity along with the increased conjugation exhibited by this cyclometalating ligand weakens the metal–ligand interaction, thereby rendering each of the series III complexes susceptible to irreversible reduction.^{33,68} Collectively, the first one-electron reduction potentials across all three series of molecules were in the range of -1.97 to -2.56 V, depending upon the specific cyclometalating ligands. These values were completely invariant (within experimental error) within each series of molecules, irrespective of the nature of the bridging pyrazolate ligand. These observations leave little doubt that in every instance the first reduction is localized on the cyclometalating ligand.

Oxidative cyclic voltammetry studies performed in THF revealed irreversible processes in every single molecule regardless of the C[^]N ligand or bridging pyrazolate moiety. Therefore, the associated ground-state oxidation potentials acquired in THF were ascertained by DPV and are collected in Table 1. The measured values here are in close agreement with the reported oxidation potentials of closely related pyrazolate-bridged binuclear platinum(II) complexes of type C[^]NPt(μ -pz)₂PtC[^]N, where C[^]N = 2-(4',6'-difluorophenyl)pyridinato-N,C^{2'}.⁶⁴ The irreversibility of the first oxidation process is not surprising, given the fact that the square-planar platinum centers are highly susceptible to nucleophilic attack by coordinating solvents, resulting in permanent oxidative addition products.^{33,64,69} The first oxidation process occurring in each Pt(II) dimer series systematically becomes easier (>100 mV variance) with increasing steric bulk accumulated on the 3,5-

positions of the pyrazolate bridges (Table 1). The increase in steric bulk in the bridging ligands results in an increased Pt–Pt σ interaction along their respective z axes, resulting in a profound impact on the electrochemical oxidation of the molecules. In the interest of harnessing potential excited-state redox chemistry from such molecules, we also performed cyclic voltammetry studies in noncoordinating CH₂Cl₂ to see if the irreversible oxidative processes observed in THF could be rendered completely reversible, potentially paving the way for multielectron reversible oxidative chemistry as a result of having two proximate Pt(II) centers. In several instances, particularly in those molecules possessing the strongest Pt–Pt interactions, the cyclic voltammograms in CH₂Cl₂ became completely reversible, exhibiting the characteristics of a one-electron oxidation. A representative example of such reversible electrochemical behavior is presented for 2c in Figure 4. We believe

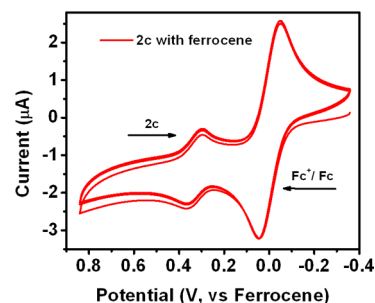


Figure 4. Cyclic voltammogram for oxidation of 2c in argon-saturated 0.1 M TBAPF₆ in dichloromethane. A platinum disk was used as the working electrode, platinum wire as the counter electrode, and silver wire as the reference electrode.

this experimental observation is completely consistent with a ground-state electronic structure featuring frontier HOMO orbitals dominated by a σ interaction occurring between the two Pt(II) centers. In essence, the irreversible oxidation processes normally exhibited in mononuclear Pt(II) complexes can be made reversible by adopting a dinuclear A-frame structure, in agreement with that previously suggested by Thompson and co-workers in related structures. Considering that the LUMO's in each series are fixed as ascertained by the reductive electrochemistry discussed above, the pyrazolate bridge-sensitive HOMO in each molecule fine-tunes the spectroscopic properties exhibited by these chromophores, as discussed in detail below.

Electronic Spectroscopy. The UV–vis absorption spectra all of 3 series of molecules measured in THF at room temperature are presented in Figure 5, and all of the relevant associated data are collected in Table 2. In all instances, the higher energy features and more intense absorption bands below 350 nm are assigned to π – π^* ligand-centered (LC) transitions, ascertained by direct comparison with each respective uncoordinated ligand (see the Supporting Information). On the basis of assignments in related molecules,⁴² the lowest energy features between 350 and ~500 nm in the electronic spectra are attributed to charge-transfer (CT) transitions terminating onto the π^* LUMOs of each respective C[^]N ligand in the three series of complexes. In instances where there is little to no steric bulk imposed by the pyrazolate bridge, when R = H, CH₃, the low-energy absorption bands can be considered as metal-to-ligand charge transfer (MLCT) in character, since the dinuclear chromophore essentially behaves

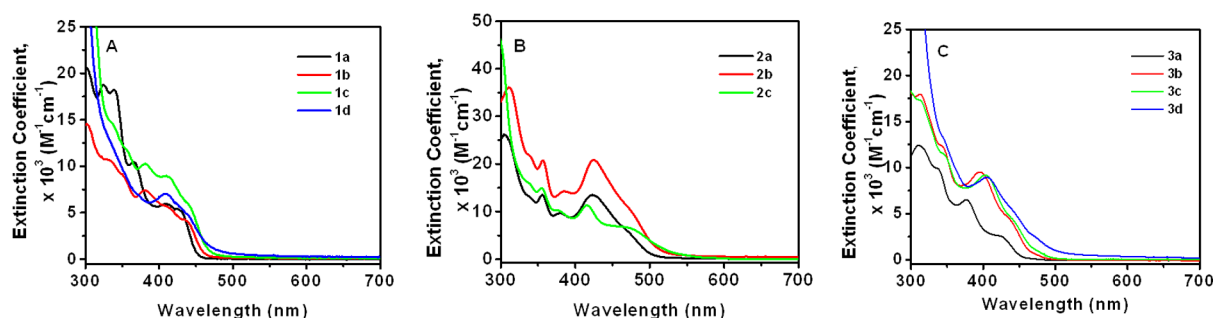


Figure 5. Absorption spectra of 1a–d (A), 2a–c (B), and 3a–d (C) measured in THF at room temperature.

Table 2. Photophysical Properties of the Pt(II) Dimers^a

complex	$\lambda_{\text{abs}}/\text{nm}$ (ϵ , $\text{M}^{-1} \text{cm}^{-1}$) ^c	$\lambda(\text{em})_{\text{rt}, 27\text{K}}$ (nm) ^e	τ_{rt} (μs) ^d	$\tau_{27\text{K}}$ (μs) ^d	τ_{TA} (μs) ^e	Φ_{em} (%) ^f	k_{r}^g (10^4 s^{-1})	k_{nr}^h (10^4 s^{-1})	ΔE_s^i (cm^{-1})
1a	300 (20483), 338 (17952), 365 (10341), 410 (5779), 430 (5197)	563, 556	18.12, 20.75			46.8	2.58	2.94	191
1b	301 (14382), 332 (10499), 351 (8942), 381 (7173), 412 (5400), 440 (3988)	565, 563	16.68, 18.4			54.0	3.24	2.76	189
1c	281 (72592), 348 (12685), 383 (9908), 412 (8627), 444 (5370)	565, 560	16.3, 17.58			57.4	3.52	2.61	184
1d	276 (52911), 410 (6931), 440 (4725)	561, 560	11.8, 16.97			61.5	5.53	3.47	96
2a	310 (25600), 355 (13204), 378 (9363), 423 (13204), 470 (6087)	604, 603	0.46, 3.83		0.44	1.9	4.13	213	82
2b	310 (35671), 355 (20303), 384 (14036), 425 (20442), 474 (10417)	610, 603	0.33, 4.00		0.34	1.3	3.94	300	250
2c	297 (45572), 355 (14699), 378 (10021), 417 (11237), 478 (6273)	713, 596	0.28, 5.83		0.26	5.6	20.0	337	3453
3a ^b	314 (12159), 337 (9778), 374 (6381), 424 (2492)	575, 486	0.53, 166.7		0.52	6.0	11.3	177	3227
3b	314 (17851), 341 (12226), 395 (9252), 440 (3957)	596, 489	0.24, 111.7		0.22	2.8	11.6	405	3588
3c	310 (17445), 346 (11283), 403 (9037), 448 (3678)	605, 490	0.66, 83		0.62	9.0	13.6	138	4408
3d	346 (12768), 406 (8740), 448 (4626)	631, 539	1.49, 7.12		1.51	19.0	12.7	54.4	3366

^aRoom-temperature and low-temperature measurements were performed in THF or MTHF respectively, unless otherwise noted. ^bRoom-temperature measurements and absolute quantum yield determinations were performed in toluene because of decomposition in ether-based solvents. ^cAbsorption and emission maxima, ± 2 nm. ^dIntensity decays, $\pm 5\%$. ^eTA decays were measured at multiple wavelengths and were finally averaged. ^fAbsolute quantum yields, $\pm 5\%$. ^g $k_{\text{r}} = \Phi/\tau$. ^h $k_{\text{nr}} = (1 - \Phi)/\tau$. ⁱ $\Delta E_s = E_{0-0}(77 \text{ K}) - E_{0-0}(298 \text{ K})$.

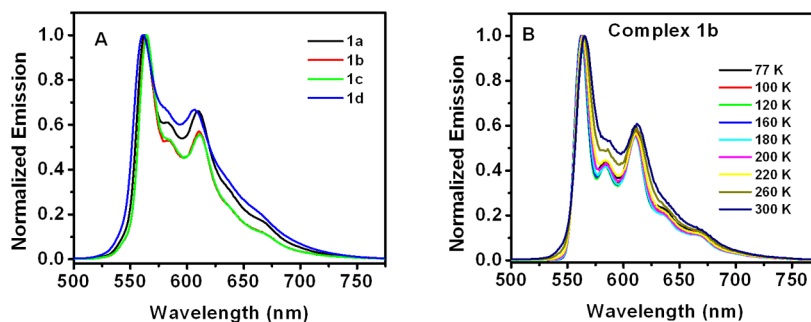


Figure 6. (A) Photoluminescence spectra of the series I chromophores measured in degassed THF at room temperature. λ_{ex} : 430 nm (1a); 440 nm (1b); 443 nm (1c); 450 nm (1d). (B) Photoluminescence spectra of 1b measured as a function of temperature in MTHF. $\tau_{\text{ex}} = 440$ ns.

like two independent mononuclear complexes.⁵⁰ However, when larger substituents are incorporated onto the 3,5-positions of the bridging pz ligands (when R = ⁱPr, phenyl), the resulting A-frame topology produces significant metal–metal σ interactions markedly affecting the electronic structure of the frontier HOMO levels, ascertained in part by the electrochemical experiments described above. Therefore, in these instances, the charge-transfer process is best described as being metal–metal-to-ligand charge transfer (MMLCT) in character; hence, the absorption bands red-shift in series II and series III with increasing steric bulk in the 3,5-substituted μ -pz ligands. This effect is observed for the lowest energy absorption band/shoulder centered at ~ 470 nm in series II, where we can

find that absorption for the most sterically hindered complex 2c tailed beyond 500 nm. Similarly, as we moved across series III from 3a to 3d, there was a small but progressive red shift in the shoulder centered around ~ 450 nm. These defining characteristics can be readily inferred from the electronic spectra provided in Figure 5.

Photoluminescence Spectroscopy. The photoluminescence spectra of all of the molecules of series I measured in degassed THF at room temperature are presented in Figure 6A. The photoluminescence profiles are almost completely invariant with respect to one another within experimental error, with the exception of slight intensity differences in the intermediate vibronic structure and the somewhat bluer-

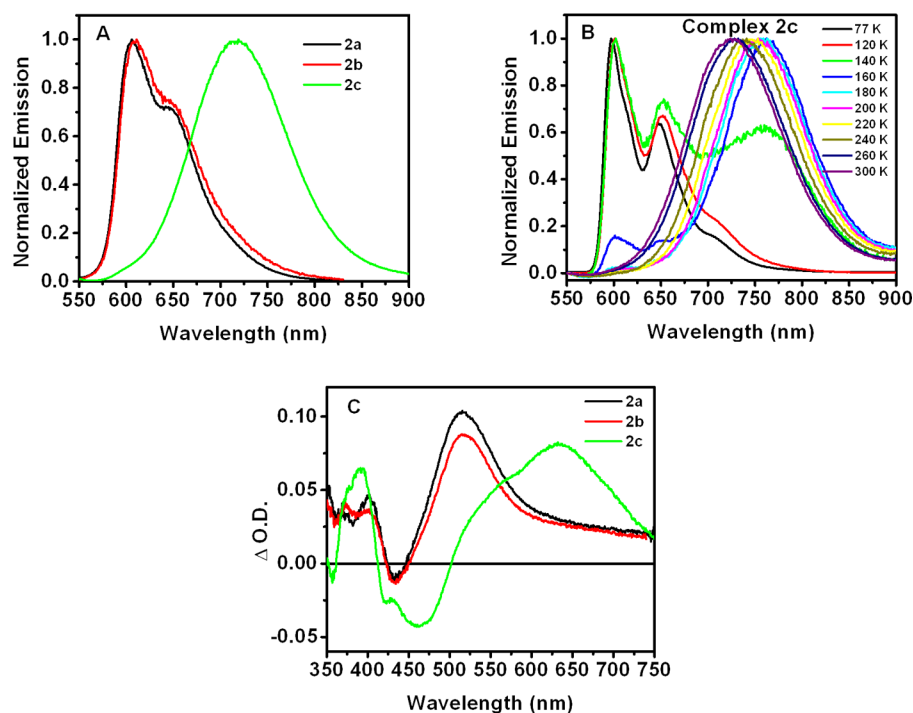


Figure 7. (A) Photoluminescence spectra of series II at room temperature in THF. (B) Photoluminescence spectra of **2c** measured as a function of temperature in MTHF. $\tau_{\text{ex}} = 478$ nm. (C) Transient absorption difference spectra of the series II chromophores measured in degassed THF at room temperature following 472 nm (**2a**), 475 nm (**2b**), or 478 nm (**2c**) pulsed laser excitation (3–4 mJ/pulse, 5–7 ns fwhm) measured at 20 ns delay time. Each difference spectrum represents the average of 64 transients.

emitting **1d**. This result immediately suggests that the nature of the emissive excited state at room temperature is precisely the same across this series. Similarly, the 77 K spectra measured in MTHF glasses exhibit similar spectral characteristics in comparison to those measured for the identical corresponding chromophore at room temperature (see the Supporting Information and Table 2). As a representative example, the temperature-dependent photoluminescence spectra of **1b** are presented in Figure 6B, which emulates the same photoluminescence behavior observed in each chromophore in series I. The vibronic progression of the emission spectrum sharpened slightly at lower temperatures, but no significant hypsochromic shift was observed, as the solution was frozen into the rigid matrix at temperatures at and below the T_g of MTHF. Such temperature-dependent emission characteristics are consistent with an excited state that is relatively nonpolar and is quite unlikely charge transfer in nature. The magnitude of the thermally induced Stokes shift ($\Delta E_s = E_{00}(77\text{ K}) - E_{00}(300\text{ K})$) has been previously utilized as a metric in elucidating the nature of the lowest lying excited state in Pt(II) charge-transfer chromophores as a function of temperature.^{52,53,70–76} Applying this tool to the molecules of series I produced a single value of $\sim 190\text{ cm}^{-1}$ for **1a–c** and 96 cm^{-1} for **1d**, thereby yielding a clear-cut assignment of thpy ligand-centered (LC) emission for all of the complexes of this series based solely on the magnitude of ΔE_s . The excited-state lifetimes for these molecules at room temperature and 77 K lie well beyond those typically measured in triplet Pt(II) charge transfer excited states (Table 2), and the values obtained in **1a–c** closely paralleled one another ($\tau_{\text{rt}} = 16.3\text{--}18\text{ }\mu\text{s}$), whereas that for **1d** was somewhat shorter ($\tau_{\text{rt}} = 11.8\text{ }\mu\text{s}$) than for the other three molecules at room temperature. The latter may be incorporating a small fraction of triplet charge-transfer character that effectively shortens its

excited-state lifetime in comparison to the other molecules of series I. In all instances, the single-exponential room-temperature luminescence intensity decays are entirely consistent with a thpy ^3LC excited state. Within the thpy dimer series, the excited-state lifetime was also largely invariant to changes in temperature (τ changed by <15% in the most extreme case), indicating that the nature of the excited state remains constant between room temperature and 77 K. As already implied by the other photoluminescence data presented above, the lowest excited state in series I at all temperatures between room temperature and 77 K is attributed to a thpy ^3LC excited state and the nature of the bridging pz ligand has no profound effect on the resultant photophysics in this series of chromophores.

Although not as structured as the photoluminescence observed in **1a–d**, the room-temperature emission spectra of the piq-containing **2a,b** in THF each exhibit vibronic side bands in their profiles, whereas that of **2c** is completely structureless and is significantly red-shifted in comparison (Figure 7A). The recorded ΔE_s values for both **2a** and **2b** are quite small, 82 and 250 cm^{-1} , respectively, reminiscent of ^3LC excited states at all temperatures between room temperature and 77 K, whereas the corresponding value in the Ph_2pz -containing **2c** ($\Delta E_s = 3453\text{ cm}^{-1}$) is more characteristic of the rigidochromic behavior of a polar charge transfer excited state (Figure 7B). Moreover, the low-temperature emission spectrum of **2c** has the same structured appearance as those of **2a,b**. Interestingly, the excited-state lifetimes in these series II chromophores measured using transient photoluminescence spectroscopy range between 280 and 460 ns at room temperature (Table 2), each entirely consistent with lifetimes exhibited in many classes of Pt(II) charge transfer excited states,^{40,77} while much shorter than those exhibited by the series I chromophores. The radiative decay rate constants (k_r) of **2a,b** were similar to those of series

I; however, that of **2c** is approximately 5 times greater, indicative of charge-transfer character. The corresponding lifetimes determined at 77 K in MTHF glasses are also quite consistent with those typically exhibited in related mononuclear Pt(II) charge-transfer chromophores.³³ The ambiguity regarding the nature of the lowest energy excited state within this series was addressed by studying time-resolved electronic absorption spectroscopy. Nanosecond transient absorption difference spectra for complexes **2a–c** were acquired in THF at room temperature (Figure 7C). The single-exponential kinetics exhibited by the transient absorption decays for all of the complexes of this series were identical across each respective difference spectrum (see the Supporting Information) and were in perfect agreement with the values determined from time-resolved photoluminescence decay measurements (Table 2). The resulting difference spectra for **2a,b** were almost identical, having a small bleach at ~430 nm and excited state absorptions centered near 400 and 525 nm. In contrast, **2c** displayed a distinct ground-state bleaching feature at 480 nm, consistent with the depletion of the ¹CT character upon formation of the excited state, followed by a substantial red shift in the primary transient absorption feature now present at 630 nm. The key spectroscopic feature in the difference spectrum in **2c** is the prevalent ground-state bleach characteristic of that expected from the formation of a CT excited state. Specifically, the combination of **2c**'s broad and structureless luminescence spectrum that exhibits strong rigidochromism possessing a large ΔE_s value, along with its characteristic transient difference spectrum and excited state decay parameters, strongly suggest that this excited state is likely ³CT in nature. However, the combined photophysical data acquired for **2a,b** is more illustrative of that expected from ³LC states. Both the photoluminescence and transient absorption studies revealed that increasing steric strain by the introduction of the 3,5-phenyl groups in the bridging pz ligands of **2c** substantially impacted the photophysics of this chromophore with respect to that of **2a,b**. This dramatic change in photophysical behavior can be accounted for as a consequence of an enhanced metal–metal interaction in **2c**, effectively altering the energetic ordering of ³LC and ³CT in this molecule. This enhancement of the Pt–Pt interaction results in significant destabilization of the frontier $d\sigma^*$ orbital, as represented in Figure 1. As a result, the HOMO should now be considered as metal–metal in character, whereas the LUMO remains fixed on the cyclometalated ligand π^* orbital. The lowest energy CT transition in **2c** is therefore termed MMLCT and its ³CT excited state can be characterized specifically as ³MMLCT. As the HOMO is $d\sigma^*$ in nature, formation of the MMLCT excited state is expected to result in a transient increase in the Pt–Pt bond order by 0.5. This type of bond shortening process has been experimentally observed previously by Gray and co-workers in $[\text{Pt}_2(\text{H}_2\text{P}_2\text{O}_5)_4]^{4-}$.^{50,67,78–81}

Similar to the case for **2c**, room-temperature emission profiles of the 7,8-benzoquinoline-containing **3b–d** in THF are broad and structureless, suggesting a polar charge-transfer excited state (Figure 8). The higher energy shoulders in **3a** likely arise from a nearby ³LC state in thermal equilibrium with the ³CT state.

The temperature dependence of the photoluminescence spectra in series III was evaluated, and the data acquired for **3b** are given in Figure 9A and are intended to be representative of the entire series. Every compound exhibits a dramatic change in its respective emission profile at temperatures below T_g of the

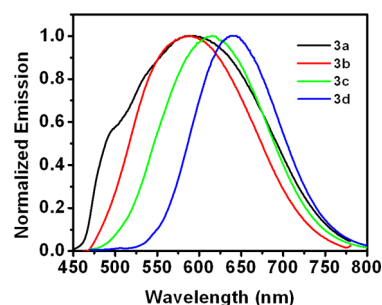


Figure 8. Photoluminescence spectra of the series III chromophores measured in degassed THF at room temperature. τ_{ex} : 400 nm (**3a**); 440 nm (**3b**); 443 nm (**3c**); 450 nm (**3d**). **3a** was recorded in toluene.

MTHF matrix, progressing from structureless above T_g to a bathochromically shifted structured emission profile below T_g (Figure S4, Supporting Information), except for the emission of **3d**, which remains quite broad at all measured temperatures. The recorded ΔE_s values in series III (Table 2) are consistent with a polar charge-transfer excited state at room temperature and suggest a possible crossover from ³CT at room temperature to ³LC at 77 K as $\Delta E_s > 3200 \text{ cm}^{-1}$. This potential change in the nature of the excited state was further supported by time-resolved photoluminescence decay measurements performed at room temperature and 77 K (Figure 9B and Table 2). The excited-state lifetimes of **3a–d** at room temperature range between 0.24 and 1.49 μs , each consistent with typical lifetimes of Pt(II) charge-transfer excited states. The excited-state lifetimes of **3a–c** at 77 K are considerably longer than those at room temperature, ranging from 83 to 166 μs , whereas that of **3d** only moderately increased to 7.1 μs . The latter observation likely results from remnant ³CT character at 77 K that shortens the excited-state lifetime in comparison to the other entries of series III. The radiative decay rate constants (k_r) of **3a–d** at room temperature were similar to each other in magnitude and were 3–4 times larger than those of series I, thereby suggesting charge transfer character in the lowest lying emissive state for each molecule at room temperature (Table 2). Transient absorption difference spectra were recorded for all the complexes in this series, and the single-exponential kinetics exhibited by the transient absorption features were quantitatively identical with those measured in the corresponding photoluminescence intensity decays. The difference spectra acquired for **3b–d** possess a significant ground-state bleach (~410 nm) in the region of the charge-transfer absorption band (similar to the case for **2c**) and an excited-state absorption centered near ~510 nm. The difference spectrum of **3a** differs from those of **3b–d**, having excited-state absorptions centered at 400, 450, and 500 nm. The photophysical behavior cited above leads to the conclusion that the lowest energy emissive state at room temperature for **3b–d** is indeed ³CT in nature. Additionally, the room-temperature photoluminescence data revealed the broad unstructured emission shifted to progressively lower energy as the steric bulk in the bridging pz ligand was increased along the series, consistent with that observed previously.^{50,67} Thus, the same reasoning leads us to the conclusion that the lowest energy excited state at room temperature for **3b–d** is best characterized as ³MMLCT in nature. As **3a** is expected to exhibit the largest Pt–Pt separation in this series, the higher energy shoulder observed in its emission profile probably arises due to the presence of a thermal equilibrium between ³LC and ³MLCT states at room

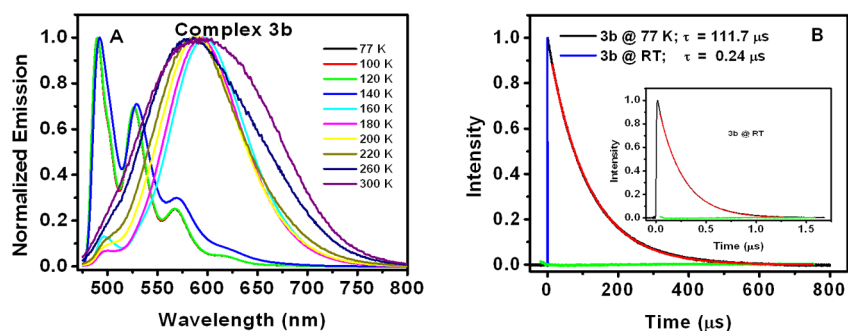


Figure 9. Temperature dependence of photoluminescence (A) and photoluminescence intensity decay (B) of 3b in MTHF.

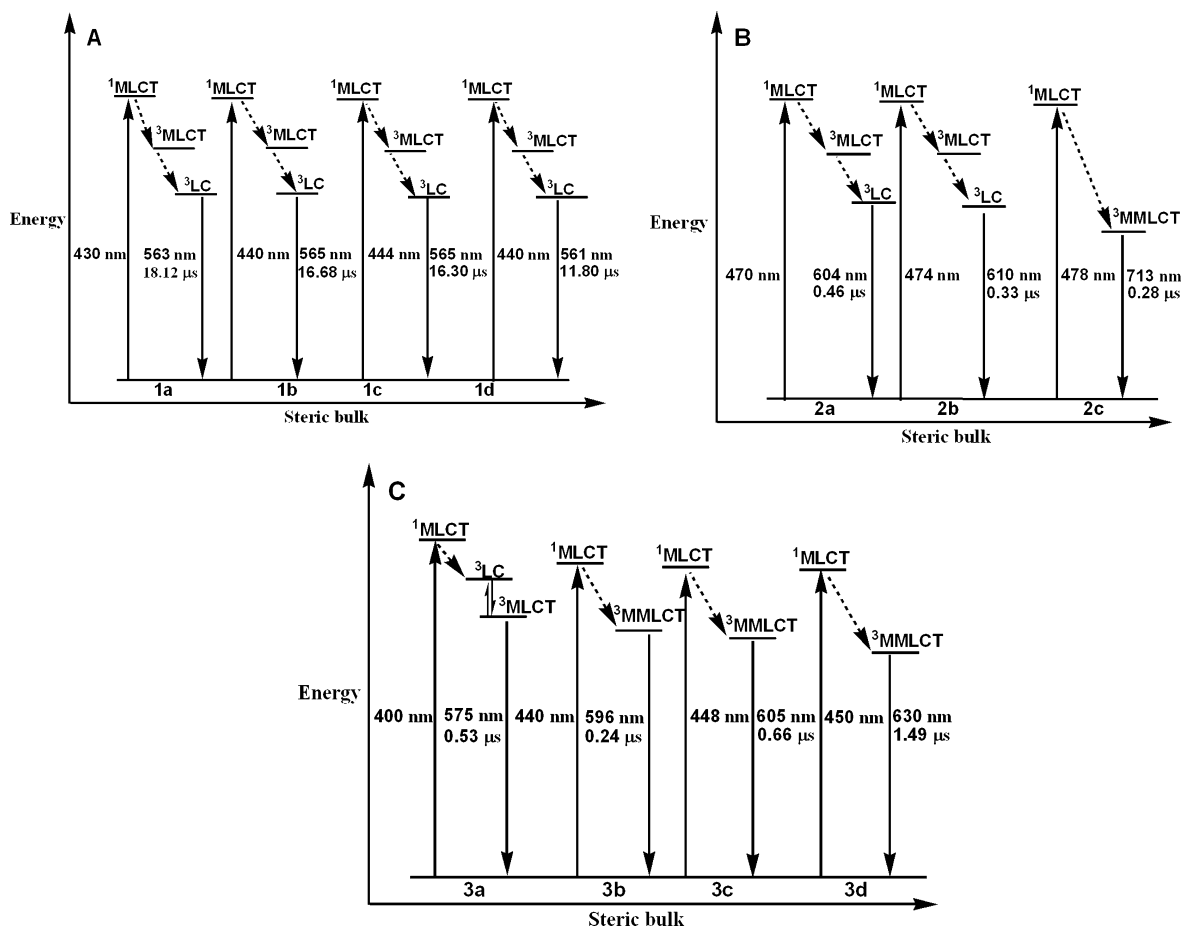


Figure 10. Energy level diagram describing the photophysical processes of series I (A), series II (B), and series III (C) Pt(II) dimer chromophores at room temperature. Solid lines represent radiative transitions, and dashed lines represent nonradiative transitions.

temperature. A synopsis compiling the qualitative Jablonski diagrams for the three series of the Pt(II) dimers at room temperature is presented in Figure 10.

CONCLUSIONS

In summary, three classes of pyrazolate-bridged platinum(II) dimers were synthesized and thoroughly characterized. Most of these complexes were isolated as a mixture of *cis* and *trans* isomers, having the *trans* form as the major product. Electrochemical studies revealed that most of these complexes exhibited two reductions which were cyclometalating ligand-centered in nature. In contrast, one-electron irreversible oxidation of platinum was observed in coordinating tetrahydrofuran whose oxidation potential was found to decrease with

increasing steric bulk in the pz bridge. However, cyclic voltammetry performed in noncoordinating dichloromethane resulted in reversible one-electron-based oxidations in most instances, indicative of the coupled metal–metal nature of the ground-state electronic structure. The photophysical properties of these complexes were tuned by substitution in the bridging pyrazolate ligands. Introduction of steric bulk in the pz bridges resulted in a change of HOMO–LUMO energy gap among the dimers of series III and 2c, which was manifested by the change of emission energy, lifetime, and quantum yield; 2c had the lowest energy gap and hence was the most red-shifted among all the dimers investigated. The nature of cyclometalating ligands also played an important part in controlling the photophysical behavior. Time-resolved photoluminescence

studies at both room temperature and 77 K along with nanosecond transient absorption spectroscopy aided in distinguishing the nature of lowest energy excited states in these chromophores. All the complexes of series I displayed ³LC-based excited states at all temperatures, while an increase of steric bulk in the pz bridge in the two other molecular series resulted in a variation of photophysical behavior ranging from charge transfer to ligand localized, including admixture behavior. The excited-state behavior of these chromophores appear most suitable for a myriad of fundamental and applied electron- and energy-transfer studies.

EXPERIMENTAL SECTION

General Considerations. All reagents purchased from commercial suppliers were used without any further purification. The compounds 7,8-benzoquinoline, 2-(2'-thienyl)pyridine, silver trifluoromethanesulfonate, potassium tetrachloroplatinate(II), 3,5-dimethylpyrazole, and 3,5-diphenylpyrazole were purchased from Aldrich Chemical Co.. Pyrazole was purchased from Alfa Aesar, and 1-phenylisoquinoline was obtained from TCI. 3,5-Diisopropylpyrazole and Pt(DMSO)₂Cl₂ were prepared by following established literature procedures.^{82,83} ¹H NMR spectra were recorded with a Bruker Advance III 500 (500 MHz) spectrometer. All chemical shifts were referenced to residual solvent signals. MALDI-TOF mass spectra were measured by a Bruker-Daltonics Omnicflex spectrometer. Elemental analyses were performed in house using a Perkin-Elmer 2400 CHN Elemental Analyzer. ESI-MS measurements were performed at the Michigan State University Mass Spectrometry Facility.

General Synthetic Procedure for the Preparation of Pt(II) Dimers. All of the reactions were performed under an inert atmosphere using standard Schlenk techniques. The intermediate cyclometalated dichloride-bridged platinum(II) dimers were prepared following a literature protocol with slight modification,³³ which involved refluxing Pt(DMSO)₂Cl₂ with 2.5 equiv of the respective cyclometalating ligand in a mixture of 2-ethoxyethanol and water (3/1) overnight. The reaction mixture was concentrated, and the product was precipitated by the addition of a water/ethanol (1/1) mixture. The solid obtained was filtered and dried under vacuum. In most cases, these dichloro-bridged dimers were not purified or characterized and were directly utilized for the synthesis of the title complexes.^{33,84–86} The pyrazolate-bridged dimers were synthesized by adapting a literature procedure.⁶³ Most of these complexes are new, although **1a** and **3a** have been previously reported by Che and co-workers.⁴² Briefly, each dichloro-bridged platinum(II) dimer was dissolved in 100 mL of 1,2-dichlorobenzene and 2 equiv of the respective pyrazolate was then added, followed by the addition of at least 2 equiv of silver triflate and a few drops of tributylamine. The reaction mixture was refluxed under argon for 30 min, and the AgCl precipitate was removed by filtration through a pad of alumina. The filtrate was concentrated, and the solid product was precipitated by addition of 1/1 ethanol/hexane and finally collected by vacuum filtration. The resultant dimer was purified by recrystallization from a suitable solvent and finally washed with pentane and dried. In most instances, the dimers were isolated as a mixture of *cis* and *trans* isomers (relative to the position of each C^N ligand in the dimer), with the *trans* form (the two C^N ligands have their C's and N's *trans* to each other) as the predominant product: *trans:cis* ≈ 2:1. All attempts to separate these two isomers were unsuccessful; however, the mixture of these two isomers had no impact whatsoever on the photophysical properties.

[Pt(thpy)(μ-H₂pz)]₂ (1a). Yield: 44% (119 mg). The solid was recrystallized from DCM/hexane and washed with pentane. The compound was isolated as a mixture of *cis* and *trans* isomers. ¹H NMR (500 MHz, CD₂Cl₂; ppm): 8.31 *cis* and 8.15 *trans* (dd, 2H total), 7.78 (dd, 2H), 7.71 (dt, 2H), 7.62 (dd, 2H), 7.42 *trans* and 7.40 *cis* (d, 2H total), 7.37 (dd, 2H), 6.90-*trans* and 6.79 *cis* (d, 2H total), 6.87 (dt, 2H), 6.56 *cis*, 6.45 *trans* and 6.34 *cis* (t, 2H total). MALDI-TOF MS: *m/z* 844. Anal. Calcd (found) for C₂₄H₁₈N₆S₂Pt₂·0.25C₆H₄Cl₂: C, 34.75 (34.49); H, 2.17 (2.11); N, 9.53 (9.51).

[Pt(thpy)(μ-Me₂pz)]₂ (1b). Yield: 37% (87 mg). The solid was recrystallized from THF/DCM and washed with pentane. The compound was isolated exclusively as the *trans* isomer. ¹H NMR (500 MHz, CD₂Cl₂; ppm): 8.07 (dd, 2H), 7.65 (dt, 2H), 7.32 (d, 2H), 7.29 (dd, 2H), 6.80 (dt, 2H), 6.72 (d, 2H), 6.05 (s, 2H), 2.30 (s, 6H), 2.25 (s, 6H). MALDI-TOF MS: *m/z* 900. Anal. Calcd (found) for C₂₈H₂₆N₆S₂Pt₂·0.25CH₂Cl₂·0.25C₄H₈O: C, 37.37 (37.60); H, 3.06 (2.78); N, 8.94 (8.64).

[Pt(thpy)(μ-ⁱPr₂pz)]₂ (1c). Yield: 41% (163 mg). The solid was recrystallized from DCM/hexane. The compound was isolated as a mixture of *cis* and *trans* isomers. ¹H NMR (500 MHz, THF-*d*₆; ppm): 8.20 *cis* and 8.04 *trans* (dd, 2H total), 7.69 (dt, 2H), 7.28 (d, 2H), 7.26 (dd, 2H), 6.83 (dt, 2H), 6.64 *trans* and 6.56 *cis* (d, 2H total), 6.12 *cis*, 6.04 *trans* and 5.96 *cis* (t, 2H total), 3.30 (m, 4H), 1.32 (d, 12H), 1.23 (d, 12H). MALDI-TOF MS: *m/z* 1012. Anal. Calcd (found) for C₃₆H₄₂N₆S₂Pt₂: C, 42.68 (42.72); H, 4.18 (4.07); N, 8.30 (8.11).

[Pt(thpy)(μ-Ph₂pz)]₂ (1d). Yield: 52% (170 mg). The solid was recrystallized from DCM/ethanol and washed with pentane. The compound was isolated as a mixture of *cis* and *trans* isomers. ¹H NMR (500 MHz, THF-*d*₆; ppm): 8.69 *cis* and 8.64 *trans* (dd, 4H total), 8.49 *trans* and 8.43 *cis* (dd, 4H total), 8.07 *cis* and 8.00 *trans* (dd, 2H total), 7.55 (m, 4H), 7.33–7.12 (m, 14H), 7.01 (d, 2H), 6.54 (dt, 2H), 6.41 *trans* and 6.38 *cis* (d, 2H total). MALDI-TOF MS: *m/z* 1149. Anal. Calcd (found) for C₄₈H₃₄N₆S₂Pt₂·C₆H₄Cl₂: C, 50.04 (49.74), H, 2.96 (2.78), N, 6.48 (6.40).

[Pt(piq)(μ-Me₂pz)]₂ (2a). Yield: 52% (180 mg). The solid was recrystallized from DCM/ethanol and washed with pentane. The compound was isolated as a *cis/trans* mixture. ¹H NMR (500 MHz, CD₂Cl₂; ppm): 8.84 (d, 2H), 8.35 *cis* and 8.22 *trans* (d, 2H total), 8.00 (dd, 2H), 7.79 (dd, 2H), 7.74 (dt, 2H), 7.65 (dt, 2H), 7.34 (dd, 2H), 7.15 (dd, 2H), 7.07 (dt, 4H), 6.12 *cis*, 6.09 *trans* and 6.07 *cis* (s, 2H total), 2.30 (s, 6H), 2.23 (s, 6H). MALDI-TOF MS: *m/z* 988. HRMS-ESI: found 989.2198 (MH⁺), calcd for C₄₀H₃₅N₆Pt₂ 989.2219.

[Pt(piq)(μ-ⁱPr₂pz)]₂ (2b). Yield: 33% (150 mg). The solid was recrystallized from THF/ethanol and washed with pentane. The compound was isolated only as the *trans* isomer. ¹H NMR (500 MHz, CD₂Cl₂; ppm): 8.84 (d, 2H), 8.16 (d, 2H), 7.98 (dd, 2H), 7.79 (dd, 2H), 7.74 (dt, 2H), 7.65 (dt, 2H), 7.31 (dd, 2H), 7.10 (dd, 2H), 7.05 (dt, 4H), 6.07 (s, 2H), 3.34 (m, 2H), 3.10 (m, 2H), 1.29 (d, 6H), 1.24 (d, 12H), 1.16 (d, 6H). MALDI-TOF MS: *m/z* 1100. HRMS-ESI: found 1101.3519 (MH⁺), calcd for C₄₈H₅₁N₆Pt₂ 1101.3471.

[Pt(piq)(μ-Ph₂pz)]₂ (2c). Yield: 61% (314 mg). The solid was recrystallized from THF/ethanol and washed with pentane. The compound was isolated as a mixture of *cis* and *trans* isomers. ¹H NMR (500 MHz, CD₂Cl₂; ppm): 8.76 *cis* and 8.73 *trans* (d, 2H total), 8.59 *cis* and 8.57 *trans* (dd, 4H total), 8.36 (dd, 4H), 8.24 (d, 2H), 7.89 *cis* and 7.85 *trans* (d, 2H total), 7.66 (dd, 4H), 7.58 (dt, 2H), 7.34–7.12 (m, 14H), 7.06 (dd, 4H), 6.91 (dt, 2H), 6.84 (dt, 2H). MALDI-TOF MS: 1236. HRMS-ESI: found 1237.2889 (MH⁺), calcd for C₆₀H₄₃N₆Pt₂ 1237.2845.

[Pt(bzq)(μ-H₂pz)]₂ (3a). Yield: 53% (92 mg). The solid was recrystallized from DCM/hexane and washed with pentane. The compound was isolated as a *cis/trans* mixture. ¹H NMR (500 MHz, CD₂Cl₂; ppm): 8.80 *cis* and 8.67 *trans* (dd, 2H total), 8.31 (dd, 2H), 7.95 (dd, 2H), 7.79 (dd, 2H), 7.76 (d, 2H), 7.59 (dd, 2H), 7.56 (d, 2H), 7.48–7.33 (m, 6H), 6.66 *cis*, 6.57 *trans*, 6.48 *cis* (t, 2H total). MALDI-TOF MS: *m/z* 880. Anal. Calcd (found) for C₃₂H₂₂N₆Pt₂: C, 43.64 (43.37); H, 2.52 (2.38); N, 9.54 (9.19).

[Pt(bzq)(μ-Me₂pz)]₂ (3b). Yield: 49% (85 mg). The solid was recrystallized from DCM/hexane and washed with pentane. The compound was isolated as a mixture of *cis* and *trans* isomers. ¹H NMR (500 MHz, THF-*d*₆; ppm): 8.72 *cis* and 8.66 *trans* (dd 2H total), 8.31 (dd, 2H), 7.62 (d, 2H), 7.48 (d, 2H), 7.42–7.36 (m, 4H), 7.31–7.24 (m, 4H), 6.08 *cis*, 6.04 *trans*, 6.00 *cis* (s, 2H total), 2.37 (s, 6H), 2.33 (s, 6H). MALDI-TOF MS: *m/z* 937. Anal. Calcd (found) for C₃₆H₃₀N₆Pt₂·C₂H₅OH: C, 46.44 (46.62); H, 3.69 (3.35); N, 8.55 (8.55).

[Pt(bzq)(μ-ⁱPr₂pz)]₂ (3c). Yield: 40% (160 mg). The solid was recrystallized from DCM/hexane and washed with pentane. The compound was isolated as a mixture of *cis* and *trans* isomers. ¹H NMR

(500 MHz, CD₂Cl₂; ppm): 8.62 *cis* and 8.56 *trans* (dd, 2H total), 8.21 (dd, 2H), 7.64 (d, 2H), 7.37 (d, 2H), 7.26 (dd, 2H), 7.29–7.18 (m, 4H), 7.17 (dd, 2H), 6.22 *cis*, 6.16 *trans* and 6.10 *cis* (s, 2H total), 3.37 (m, 4H), 1.36 (d, 12H), 1.23 (d, 12H). MALDI-TOF MS: *m/z* 1048. HRMS-ESI: found 1049.3181 (MH⁺), calcd for C₄₄H₄₇N₆Pt₂ 1049.3158.

[Pt(bzq)(μ-Ph₂pz)]₂ (**3d**). Yield: 47% (411 mg). The solid was recrystallized from THF/ethanol. The compound was isolated as a mixture of *cis* and *trans* isomers. ¹H NMR (500 MHz, THF-*d*₆; ppm): 8.74 *trans* and 8.71 *cis* (dd, 4H total), 8.61 *cis* and 8.57 *trans* (dd, 4H total), 8.53 *trans* and 8.48 *cis* (dd, 2H total), 8.04 (dd, 2H), 7.41 (d, 2H), 7.31 (s, 2H), 7.27 (d, 2H), 7.24–7.01 (m, 20H). MALDI-TOF MS: *m/z* 1184. Anal. Calcd (found) for C₅₆H₃₈N₆Pt₂·0.5C₆H₁₄·0.5C₆H₄Cl₂: C, 57.21 (57.22); H, 3.64 (3.32); N, 6.46 (6.49).

Spectroscopic Measurements. UV–vis absorption spectra were recorded with a Cary 50 Bio UV–visible spectrophotometer from Varian. Uncorrected steady-state photoluminescence spectra at both room temperature and 77 K were measured with a single photon counting spectrofluorimeter from Edinburgh Analytical Instruments (FS920) equipped with a 450 W Xe arc lamp (Xe900) and an extended red-sensitive PMT (R2658P). The sample temperatures were controlled using an Oxford Instruments Cryostat (Optistat DN) capable of housing liquid samples in a temperature range from 77 to 300 K. Temperatures were controlled with an ITC-503 (Oxford Instruments) temperature controller. Emission lifetimes were recorded using a nitrogen-pumped broad-band dye laser as an excitation source (PTI GL3300 Nitrogen Laser, PTI GL301 dye laser) as previously described^{54,87} or using the laser flash photolysis apparatus described below operating in emission mode. A computer-controlled Nd:YAG laser/OPO system, Vibrant LD 355 II from Oportek, operating at 1 Hz was used as an excitation source for transient absorption spectroscopy. The nanosecond transient absorption difference spectra were recorded with a commercial laser flash photolysis spectrometer (LP920-K, Edinburgh Instruments) equipped with a pulsed 450 W Xe arc lamp. Solutions had an absorbance between 0.25 and 0.5 at the excitation wavelength and were degassed using multiple FPT degassing cycles. Absolute photoluminescence quantum yield measurements were performed with a Hamamatsu spectrometer (C11347), consisting of a Xe lamp/monochromator excitation source, an integrating sphere, and a back-thinned CCD detector.

Electrochemistry. Cyclic voltammetry and differential pulsed voltammetry were performed using a BAS Epsilon electrochemistry workstation in a conventional three-electrode arrangement with all experiments performed in an O₂-free and water-free glovebox (MBraun). Oxidation potentials were measured in both CH₂Cl₂ and THF solvents containing 0.1 M tetrabutylammonium hexafluorophosphate as the supporting electrolyte. A platinum disk was used as working electrode, a platinum wire as the counter electrode, and a silver wire as the reference electrode. Measurements were conducted with a scan rate of 100 mV/s, and ferrocenium/ferrocene (Fc⁺/Fc) was used as the internal standard. Reduction potentials were measured in anhydrous toluene/acetonitrile (1/1) and in anhydrous acetonitrile. Here Ag/AgNO₃ was used as the reference electrode. For all the measurements, potentials were reported vs ferrocenium/ferrocene (Fc⁺/Fc) internal standard.

■ ASSOCIATED CONTENT

Supporting Information

Text and figures giving synthetic details, electrochemical data, and static and dynamic photoluminescence spectra at various temperatures. This material is available free of charge via the Internet at <http://pubs.acs.org>.

■ AUTHOR INFORMATION

Corresponding Author

*E-mail for F.N.C.: castell@bgsu.edu.

Notes

The authors declare no competing financial interest.

■ ACKNOWLEDGMENTS

This work was supported by funding from the National Science Foundation (No. CBET-0731153) and the State of Ohio through the Ohio Research Scholars program. Dr. Catherine E. McCusker, Dr. Mykhaylo Myahkostupov, Dr. Aaron A. Rachford, and Dr. Valentina Prusakova are gratefully acknowledged for their assistance and valuable discussions.

■ REFERENCES

- (1) Zhang, D.; Wu, L. Z.; Zhou, L.; Han, X.; Yang, Q. Z.; Zhang, L. P.; Tung, C. H. *J. Am. Chem. Soc.* **2004**, *126*, 3440.
- (2) Connick, W. B.; Gray, H. B. *J. Am. Chem. Soc.* **1997**, *119*, 11620.
- (3) Hissler, M.; McGarrah, J. E.; Connick, W. B.; Geiger, D. K.; Cummings, S. D.; Eisenberg, R. *Coord. Chem. Rev.* **2000**, *208*, 115.
- (4) Wang, X. H.; Goeb, S.; Ji, Z. Q.; Pogulaichenko, N. A.; Castellano, F. N. *Inorg. Chem.* **2011**, *50*, 705.
- (5) Evans, R. C.; Douglas, P.; Winscom, C. J. *Coord. Chem. Rev.* **2006**, *250*, 2093.
- (6) Lu, W.; Mi, B. X.; Chan, M. C. W.; Hui, Z.; Che, C. M.; Zhu, N. Y.; Lee, S. T. *J. Am. Chem. Soc.* **2004**, *126*, 4958.
- (7) Wong, W. Y.; He, Z.; So, S. K.; Tong, K. L.; Lin, Z. Y. *Organometallics* **2005**, *24*, 4079.
- (8) Ma, B.; Djurovich, P. I.; Yousufuddin, M.; Bau, R.; Thompson, M. E. *J. Phys. Chem. C* **2008**, *112*, 8022.
- (9) McGarrah, J. E.; Kim, Y. J.; Hissler, M.; Eisenberg, R. *Inorg. Chem.* **2001**, *40*, 4510.
- (10) Lamansky, S.; Djurovich, P.; Murphy, D.; Abdel-Razzaq, F.; Lee, H. E.; Adachi, C.; Burrows, P. E.; Forrest, S. R.; Thompson, M. E. *J. Am. Chem. Soc.* **2001**, *123*, 4304.
- (11) Thomas, S. W.; Venkatesan, K.; Muller, P.; Swager, T. M. *J. Am. Chem. Soc.* **2006**, *128*, 16641.
- (12) Siu, P. K. M.; Lai, S. W.; Lu, W.; Zhu, N. Y.; Che, C. M. *Eur. J. Inorg. Chem.* **2003**, 2749.
- (13) Lanoe, P. H.; Fillaut, J. L.; Toupet, L.; Williams, J. A. G.; Le Bozec, H.; Guerchais, V. *Chem. Commun.* **2008**, 4333.
- (14) Wong, K. H.; Chan, M. C. W.; Che, C. M. *Chem. Eur. J.* **1999**, *5*, 2845.
- (15) Koo, C. K.; Ho, Y. M.; Chow, C. F.; Lam, M. H. W.; Lau, T. C.; Wong, W. Y. *Inorg. Chem.* **2007**, *46*, 3603.
- (16) Peyratout, C. S.; Aldridge, T. K.; Crites, D. K.; Mcmillin, D. R. *Inorg. Chem.* **1995**, *34*, 4484.
- (17) Wang, A. H. J.; Nathans, J.; Vandermaer, G.; Vanboom, J. H.; Rich, A. *Nature* **1978**, *276*, 471.
- (18) Espinet, P.; Esteruelas, M. A.; Oro, L. A.; Serrano, J. L.; Sola, E. *Coord. Chem. Rev.* **1992**, *117*, 215.
- (19) Ghedini, M.; Pucci, D.; Crispini, A.; Barberio, G. *Organometallics* **1999**, *18*, 2116.
- (20) Sun, R. W. Y.; Ma, D. L.; Wong, E. L. M.; Che, C. M. *Dalton Trans.* **2007**, 4884.
- (21) Baldo, M. A.; O'Brien, D. F.; You, Y.; Shoustikov, A.; Sibley, S.; Thompson, M. E.; Forrest, S. R. *Nature* **1998**, *395*, 151.
- (22) Vezzu, D. A. K.; Deaton, J. C.; Jones, J. S.; Bartolotti, L.; Harris, C. F.; Marchetti, A. P.; Kondakova, M.; Pike, R. D.; Huo, S. Q. *Inorg. Chem.* **2010**, *49*, 5107.
- (23) Chassot, L.; Muller, E.; Vonzelewsky, A. *Inorg. Chem.* **1984**, *23*, 4249.
- (24) Deuschelcornioley, C.; Luond, R.; Vonzelewsky, A. *Helv. Chim. Acta* **1989**, *72*, 377.
- (25) Constable, E. C.; Henney, R. P. G.; Leese, T. A.; Tocher, D. A. J. *Chem. Soc., Chem. Commun.* **1990**, 513.
- (26) Che, C. M.; Fu, W. F.; Lai, S. W.; Hou, Y. J.; Liu, Y. L. *Chem. Commun.* **2003**, 118.
- (27) Cave, G. W. V.; Alcock, N. W.; Rourke, J. P. *Organometallics* **1999**, *18*, 1801.

- (28) Lu, W.; Chan, M. C. W.; Cheung, K. K.; Che, C. M. *Organometallics* **2001**, *20*, 2477.
- (29) Cardenas, D. J.; Echavarren, A. M.; de Arellano, M. C. R. *Organometallics* **1999**, *18*, 3337.
- (30) Williams, J. A. G.; Beeby, A.; Davies, E. S.; Weinstein, J. A.; Wilson, C. *Inorg. Chem.* **2003**, *42*, 8609.
- (31) Jude, H.; Bauer, J. A. K.; Connick, W. B. *Inorg. Chem.* **2004**, *43*, 725.
- (32) Song, D. T.; Wu, Q. G.; Hook, A.; Kozin, I.; Wang, S. N. *Organometallics* **2001**, *20*, 4683.
- (33) Brooks, J.; Babayan, Y.; Lamansky, S.; Djurovich, P. I.; Tsyba, I.; Bau, R.; Thompson, M. E. *Inorg. Chem.* **2002**, *41*, 3055.
- (34) Baldo, M. A.; O'Brien, D. F.; Thompson, M. E.; Forrest, S. R. *Phys. Rev. B* **1999**, *60*, 14422.
- (35) Adachi, C.; Baldo, M. A.; Forrest, S. R.; Thompson, M. E. *Appl. Phys. Lett.* **2000**, *77*, 904.
- (36) Adachi, C.; Baldo, M. A.; Thompson, M. E.; Forrest, S. R. *J. Appl. Phys.* **2001**, *90*, 5048.
- (37) Ma, B. W.; Djurovich, P. I.; Thompson, M. E. *Coord. Chem. Rev.* **2005**, *249*, 1501.
- (38) Rausch, A. F.; Thompson, M. E.; Yersin, H. *Chem. Phys. Lett.* **2009**, *468*, 46.
- (39) Adachi, C.; Kwong, R. C.; Djurovich, P.; Adamovich, V.; Baldo, M. A.; Thompson, M. E.; Forrest, S. R. *Appl. Phys. Lett.* **2001**, *79*, 2082.
- (40) Lai, S. W.; Chan, M. C. W.; Cheung, T. C.; Peng, S. M.; Che, C. M. *Inorg. Chem.* **1999**, *38*, 4046.
- (41) Lai, S. W.; Cheung, T. C.; Chan, M. C. W.; Cheung, K. K.; Peng, S. M.; Che, C. M. *Inorg. Chem.* **2000**, *39*, 255.
- (42) Lai, S. W.; Chan, M. C. W.; Cheung, K. K.; Peng, S. M.; Che, C. M. *Organometallics* **1999**, *18*, 3991.
- (43) Bercaw, J. E.; Durrell, A. C.; Gray, H. B.; Green, J. C.; Hazari, N.; Labinger, J. A.; Winkler, J. R. *Inorg. Chem.* **2010**, *49*, 1801.
- (44) Bailey, J. A.; Gray, H. B. *Acta Crystallogr.* **1992**, *C48*, 1420.
- (45) Bailey, J. A.; Miskowski, V. M.; Gray, H. B. *Inorg. Chem.* **1993**, *32*, 369.
- (46) Wang, K. W.; Chen, J. L.; Cheng, Y. M.; Chung, M. W.; Hsieh, C. C.; Lee, G. H.; Chou, P. T.; Chen, K.; Chi, Y. *Inorg. Chem.* **2010**, *49*, 1372.
- (47) Jain, V. K.; Kannan, S.; Tiekink, E. R. T. *J. Chem. Soc., Dalton Trans.* **1993**, 3625.
- (48) Yam, V. W. W.; Yu, K. L.; Cheng, E. C. C.; Yeung, P. K. Y.; Cheung, K. K.; Zhu, N. Y. *Chem. Eur. J.* **2002**, *8*, 4121.
- (49) Roundhill, D. M.; Gray, H. B.; Che, C. M. *Acc. Chem. Res.* **1989**, *22*, 55.
- (50) Ma, B.; Li, J.; Djurovich, P. I.; Yousufuddin, M.; Bau, R.; Thompson, M. E. *J. Am. Chem. Soc.* **2005**, *127*, 28.
- (51) Castellano, F. N.; Pomestchenko, I. E.; Shikhova, E.; Hua, F.; Muro, M. L.; Rajapakse, N. *Coord. Chem. Rev.* **2006**, *250*, 1819.
- (52) Hua, F.; Kinayyigit, S.; Cable, J. R.; Castellano, F. N. *Inorg. Chem.* **2006**, *45*, 4304.
- (53) Goeb, S.; Rachford, A. A.; Castellano, F. N. *Chem. Commun.* **2008**, 814.
- (54) Rachford, A. A.; Goeb, S.; Ziesel, R.; Castellano, F. N. *Inorg. Chem.* **2008**, *47*, 4348.
- (55) Rachford, A. A.; Hua, F.; Adams, C. J.; Castellano, F. N. *Dalton Trans.* **2009**, 3950.
- (56) Huang, H.-P.; Li, S.-H.; Yu, S. Y.; Li, Y.-Z.; Jiao, Q.; Pan, Y.-J. *Inorg. Chem. Commun.* **2005**, *8*, 656.
- (57) Bushnell, G. W.; Fjeldsted, D. O. K.; Stobart, S. R.; Wang, J. J. *Organometallics* **1996**, *15*, 3785.
- (58) Torres, F.; Sola, E.; Elduque, A.; Martinez, A. P.; Lahoz, F. J.; Oro, L. A. *Chem. Eur. J.* **2000**, *6*, 2120.
- (59) Kurnikov, I. V.; Zusman, L. D.; Kurnikova, M. G.; Farid, R. S.; Beratan, D. N. *J. Am. Chem. Soc.* **1997**, *119*, 5690.
- (60) Yam, V. W. W.; Wong, K. M. C.; Zhu, N. Y. *J. Am. Chem. Soc.* **2002**, *124*, 6506.
- (61) Lai, S. W.; Lam, H. W.; Lu, W.; Cheung, K. K.; Che, C. M. *Organometallics* **2002**, *21*, 226.
- (62) Yersin, H.; Donges, D.; Humbs, W.; Strasser, J.; Sitters, R.; Glasbeek, M. *Inorg. Chem.* **2002**, *41*, 4915.
- (63) Connick, W. B.; Marsh, R. E.; Schaefer, W. P.; Gray, H. B. *Inorg. Chem.* **1997**, *36*, 913.
- (64) Ma, B.; Djurovich, P. I.; Garon, S.; Alleyne, B.; Thompson, M. E. *Adv. Funct. Mater.* **2006**, *16*, 2438.
- (65) Lockard, J. V.; Rachford, A. A.; Smolentsev, G.; Stickrath, A. B.; Wang, X. H.; Zhang, X. Y.; Atenkoff, K.; Jennings, G.; Soldatov, A.; Rheingold, A. L.; Castellano, F. N.; Chen, L. X. *J. Phys. Chem. A* **2010**, *114*, 12780.
- (66) Cho, S.; Mara, M. W.; Wang, X. H.; Lockard, J. V.; Rachford, A. A.; Castellano, F. N.; Chen, L. X. *J. Phys. Chem. A* **2011**, *115*, 3990.
- (67) Rachford, A. A.; Castellano, F. N. *Inorg. Chem.* **2009**, *48*, 10865.
- (68) Kulikova, M. V.; Balashev, K. P.; Kvam, P. I.; Songstad, J. *Russ. J. Gen. Chem.* **2000**, *70*, 163.
- (69) Kvam, P. I.; Puzyk, M. V.; Balashev, K. P.; Songstad, J. *Acta Chem. Scand.* **1995**, *49*, 335.
- (70) Chen, P. Y.; Meyer, T. J. *Chem. Rev.* **1998**, *98*, 1439.
- (71) Whittle, C. E.; Weinstein, J. A.; George, M. W.; Schanze, K. S. *Inorg. Chem.* **2001**, *40*, 4053.
- (72) Pomestchenko, I. E.; Castellano, F. N. *J. Phys. Chem. A* **2004**, *108*, 3485.
- (73) Rachford, A. A.; Goeb, S.; Castellano, F. N. *J. Am. Chem. Soc.* **2008**, *130*, 2766.
- (74) Muro, M. L.; Rachford, A. A.; Wang, X. H.; Castellano, F. N. *Top. Organomet. Chem.* **2010**, *29*, 159.
- (75) Guo, H. M.; Muro-Small, M. L.; Ji, S. M.; Zhao, J. Z.; Castellano, F. N. *Inorg. Chem.* **2010**, *49*, 6802.
- (76) Goeb, S.; Prusakova, V.; Wang, X. H.; Vezinat, A.; Salle, M.; Castellano, F. N. *Chem. Commun.* **2011**, *47*, 4397.
- (77) Yip, H. K.; Che, C. M.; Zhou, Z. Y.; Mak, T. C. W. *J. Chem. Soc., Chem. Commun.* **1992**, 1369.
- (78) Kim, C. D.; Pillet, S.; Wu, G.; Fullagar, W. K.; Coppens, P. *Acta Crystallogr.* **2002**, *A58*, 133.
- (79) Novozhilova, I. V.; Volkov, A. V.; Coppens, P. *J. Am. Chem. Soc.* **2003**, *125*, 1079.
- (80) Ozawa, Y.; Terashima, M.; Mitsumi, M.; Toriumi, K.; Yasuda, N.; Uekusa, H.; Ohashi, Y. *Chem. Lett.* **2003**, *32*, 62.
- (81) Rice, S. F.; Gray, H. B. *J. Am. Chem. Soc.* **1983**, *105*, 4571.
- (82) Wang, Z. X.; Qin, H. L. *Green Chem.* **2004**, *6*, 90.
- (83) Kukushkin, V. Y.; Pombeiro, A. J. L.; Ferreira, C. M. P.; Elding, L. I.; Puddephatt, R. J. *Inorg. Synth.* **2002**, *33*, 189.
- (84) Ghavale, N.; Wadawale, A.; Dey, S.; Jain, V. K. *J. Organomet. Chem.* **2010**, *695*, 1237.
- (85) Cave, G. W. V.; Fanizzi, F. P.; Deeth, R. J.; Errington, W.; Rourke, J. P. *Organometallics* **2000**, *19*, 1355.
- (86) Pregosin, P. S.; Wombacher, F.; Albinati, A.; Lianza, F. *J. Organomet. Chem.* **1991**, *418*, 249.
- (87) Kozlov, D. V.; Tyson, D. S.; Goze, C.; Ziesel, R.; Castellano, F. N. *Inorg. Chem.* **2004**, *43*, 6083.